

Corrosion Behavior of as-Cast Mg-6Zn-4Si Alloy with Sr Addition

Cong Mengqi¹, Li Ziquan^{1,2}, Liu Jinsong¹, Wang Menghui¹, Sheng Beibei¹, Wang Bijun¹

¹ Nanjing University of Aeronautics and Astronautics, Nanjing 210016, China; ² Nanjing Polytechnic Institute, Nanjing 210048, China

Abstract: The microstructure and corrosion resistance of Mg-6Zn-4Si alloy with Sr addition were studied using XRD, OM, SEM, EDS, potentiodynamic polarization and immersion testing. The results show that the morphologies and sizes of both the primary and eutectic Mg₂Si in Mg-6Zn-4Si alloy can be effectively modified by the Sr additions. With the increasing amount of Sr addition, the primary Mg₂Si phase experiences a decrease in the grain size with a subsequent increase. Sr significantly improves the corrosion resistance of Mg-6Zn-4Si alloy. The ternary alloy with 0.5wt%Sr has the optimal corrosion resistance, which exhibits the highest corrosion potential, the lowest corrosion current density and corrosion rate. The homogeneous dispersion of fine Mg₂Si particles with Sr element is responsible for the improvement of corrosion resistance. Excessive Sr ($\geq 1.0\text{wt}\%$) leads to the generation of SrMgSi new phase, which has unfavorable effects on the corrosion resistance of the alloys.

Key words: magnesium alloys; casting; microstructure; corrosion behavior

Recently, hyper-eutectic Mg-Zn-Si system with thermally stable Mg₂Si particles has been attracted more and more attention due to the excellent performance and potential application^[1-4]. Generally, Mg₂Si phases are inclined to form as coarse dendrite and Chinese script type under conventional solidification^[3]. To improve its mechanical properties and corrosion behavior, grain refinement in the microstructure is a good approach, and many researches have modified the primary and eutectic Mg₂Si phase via a variety of process techniques^[5,6] or alloying elements addition, such as Ca, Zn, La, Pb, and Sb^[7-10].

As an alkaline earth metals addition, strontium (Sr) is often used to refine the microstructure and improve the mechanical properties^[11,12]. Meanwhile, the addition of Sr element is also generally believed to have a beneficial influence on corrosion resistance of Mg alloy. Up to now, the effect of Sr on the corrosion resistance of magnesium alloys containing high Si has not been reported.

The aim of this paper is to study the influence of Sr on microstructure and corrosion behavior of as-cast Mg-6Zn-4Si alloy containing high Si, further to reveal the corrosion mechanisms for design of an alloy for any application.

1 Experiment

Mg-6Zn-4Si alloy was prepared by commercial Mg ingot, Zn ingot and Mg-10.14%Si master alloy in an electric resistance furnace. The entire casting process was protected by the mixed gas of 1 vol% SF₆+99 vol% Ar. In order to dissolve silicon completely, the raw materials were continuously heated to above 750 °C and kept for 20 min, and then stirred for 5 min. Finally, the melt was poured in a permanent mould with dimensions of 100 mm×80 mm×20 mm, which has been preheated to 250 °C.

Different amounts of Sr (nominally, 0.1, 0.5, 1.0, 1.5 and 2.0 wt%) were added into the remelted Mg-6Zn-4Si alloy, using a the Mg-21.4%Sr master alloy. To ensure the

Received date: September 09, 2016

Foundation item: The Funding of Jiangsu Innovation Program for Graduate Education (CXZZ13_0160); the Fundamental Research Funds for the Central Universities, Nanjing University of Aeronautics and Astronautics Research Funding (NS2013060); the Priority Academic Program Development of Jiangsu Higher Education Institutions

Corresponding author: Li Ziquan, Ph. D., Professor, College of Material Science and Technology, Nanjing University of Aeronautics and Astronautics, Nanjing 210016, P. R. China, Tel: 0086-25-52112626, E-mail: ziquanli@nuaa.edu.cn

Copyright © 2017, Northwest Institute for Nonferrous Metal Research. Published by Elsevier BV. All rights reserved.

homogeneity, the molten samples were mechanically stirred after being annealed at 750 °C for 15 min. After that, the molten samples were poured into the mould to form the as-cast samples. The specimens cut from the same position in the as-cast ingots, as shown in Fig.1, were used for the

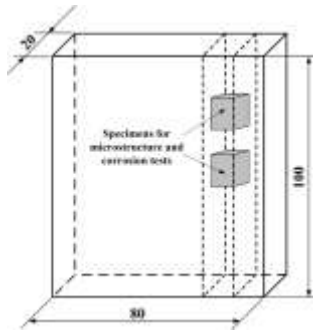


Fig.1 Positions of the cut specimens for microstructural observation and corrosion tests (mm)

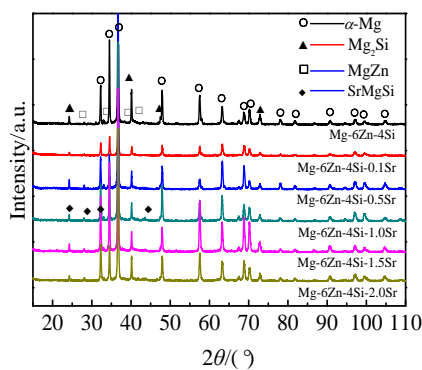


Fig.2 XRD patterns of the experimental alloys

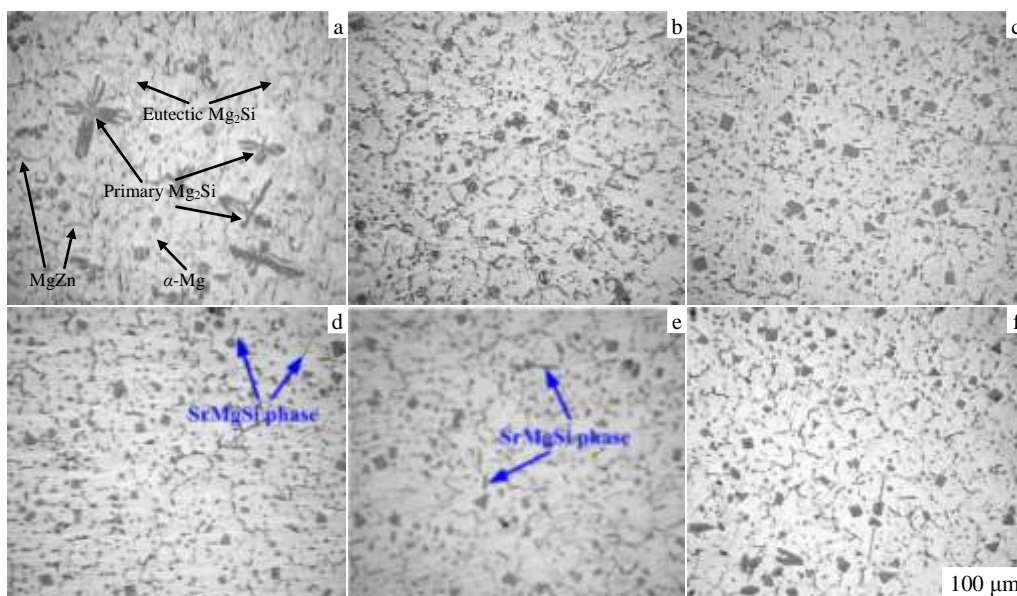


Fig.3 OM images of the as-cast Mg-6Zn-4Si-xSr alloys: (a) without Sr, (b) 0.1% Sr, (c) 0.5% Sr, (d) 1.0%Sr, (e) 1.5%Sr, and (f) 2.0%Sr

microstructural observation and corrosion tests. Further details are available in Ref. [3].

The immersion test and potentiodynamic polarization were used to assess the corrosion behavior of the experimental alloys. The dimension of the samples for corrosion testing was 10 mm×10 mm×3 mm (thickness). The specimens for immersion test were immersed in 3.5wt% NaCl solution at ambient temperature. After 36 h immersion, the corrosion products of the specimens were removed in the boiling solution of 15%Cr₂O₃+1%AgNO₃+500 mLH₂O. Potentiodynamic polarization was conducted in 3.5% NaCl aqueous solution with a polarization scan rate of 1 mV s⁻¹. The specimens were ground by 1200 grit emery paper, cleaned in acetone and then embedded leaving a square surface of 1 cm² exposed to the solution.

2 Results

2.1 Microstructural characterization

XRD results of Mg-6Zn-4Si alloys with different Sr amounts in Fig.2 indicate that a new SrMgSi phase can be found when the Sr addition is over 0.5%. Fig.3 shows the OM images of the experimental alloys. The semi-continuous network phase in Fig.3a are thought to be MgZn phase by combining analyses of SEM image, EDS (shown in Fig.4) and XRD results. From Fig.3b~3f, it can be observed that the primary Mg₂Si phase changes to polygonal or fine block particles, and the eutectic Mg₂Si changes to fine fiber with Sr addition, indicating that Sr addition can effectively modify and refine the Mg₂Si phases. The size of primary Mg₂Si observably decreases with increasing Sr up to 0.5%, and then gradually increases (shown in Fig.5). Moreover, when the Sr addition is beyond 0.5%, some needle-like particles appear, which has been determined to be SrMgSi alloy in our previous work^[13].

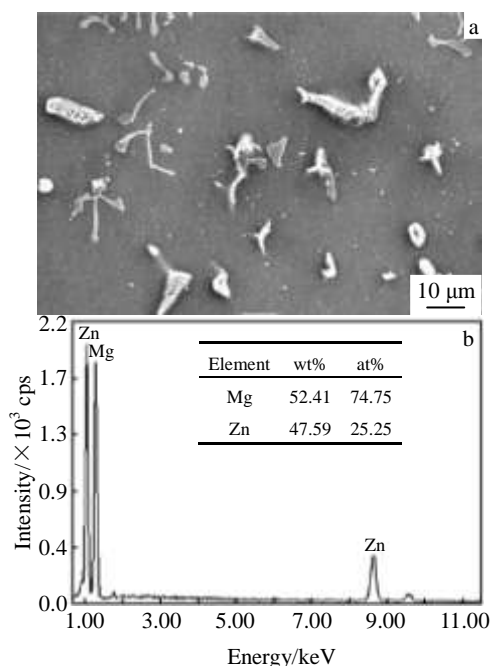


Fig.4 SEM image (a) and EDS result (b) of the semi-continuous network phase in the as-cast Mg-6Zn-4Si alloy

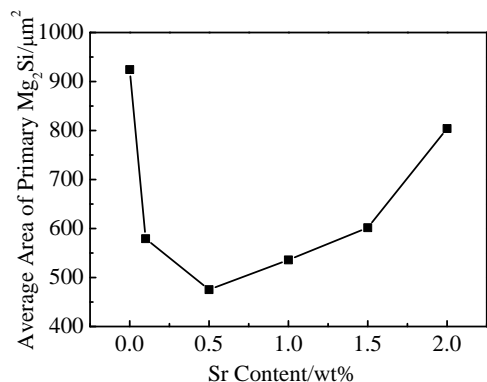


Fig.5 Relationship between Sr content and average area of primary Mg₂Si grains

2.2 Corrosion characterization

2.2.1 Potentiodynamic polarization

Fig.6 displays polarization curves of Mg-6Zn-4Si alloys without or with Sr additions at room temperature in 3.5% NaCl aqueous solution, and all polarization curves of the experimental alloys are in accord with the tafel curves. The corresponding corrosion potential (E_{corr}), the current density (I_{corr}) obtained from Fig.6 are shown in Table 1. Mg-6Zn-4Si alloy exhibits a low corrosion potential (-1.564 V) and a high current density (1.820×10^{-4} A cm^{-2}). The corrosion potential shifts observably toward more noble position after adding 0.1% and 0.5% Sr elements, and the experimental alloys have a corrosion potential of -1.553 and -1.094 V, which is approximately 0.01, 0.47 V higher than that of the base alloy, respectively. The current density of the experimental alloys decreases after adding 0.1% and 0.5% Sr elements. However, further addition of Sr content to 1.5% causes a slight decrease in the corrosion potential though it is still more positive than that of the base alloy. It is worth pointing out that the current density of Mg-6Zn-4Si alloy is one to three orders of magnitude larger than those of the alloys with Sr additions. By contrast, Mg-6Zn-4Si alloy with 0.5Sr addition shows the most favorable corrosion resistance.

2.2.2 Corrosion rate

Fig.7 shows the corrosion rates of the experimental alloys after immersion in 3.5% NaCl solution for 36 h. It can be found that the corrosion rates of the experimental alloys significantly decreases with an increase of Sr from 0.1% to 0.5%. Continued addition of Sr to 1.5% causes a slight increase of the corrosion rate. Mg-6Zn-4Si-0.5Sr alloy shows the smallest corrosion rates compared with other alloys, indicating the best corrosion resistance.

2.2.3 Corrosion morphologies

Fig.8 depicts surface SEM images with high magnification of the experimental alloys after immersion in 3.5% NaCl aqueous solution for 36 h and removal of the corrosion products. It can be seen from Fig.8a that the surface of the base alloy is covered by a corrosion layer with some large cracks and deep corrosion pits. The length of cracks and the size of corrosion pits on the surface of the alloys containing 0.1%Sr are much smaller than those of the base alloy (as shown in Fig.8b). When the amount of Sr addition is 0.5%, the

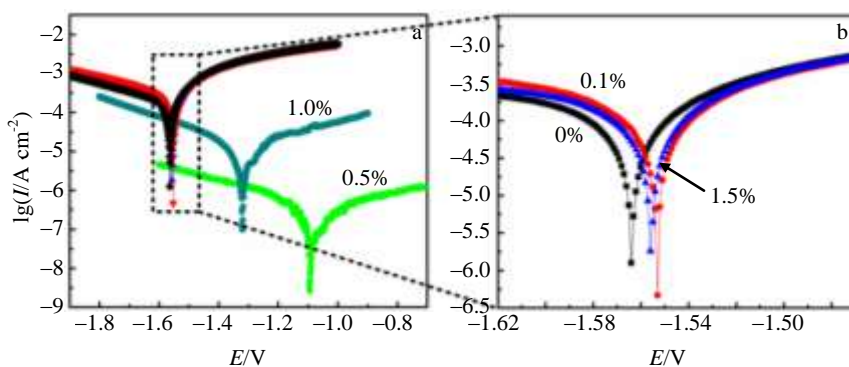


Fig.6 Polarization curves of as-cast Mg-6Zn-4Si alloys with 0.5%, 1.0% Sr additions (a) and 0, 0.1%, 1.5% Sr additions (b)

Table 1 Electrochemical corrosion data of the experimental alloys

Metallurgy designation	E_{corr}/V	$I_{\text{corr}}/A \text{ cm}^{-2}$
0	-1.564	1.820×10^{-4}
0.1Sr	-1.553	1.785×10^{-4}
0.5Sr	-1.094	1.514×10^{-7}
1.0Sr	-1.320	5.623×10^{-6}
1.5Sr	-1.556	2.209×10^{-4}

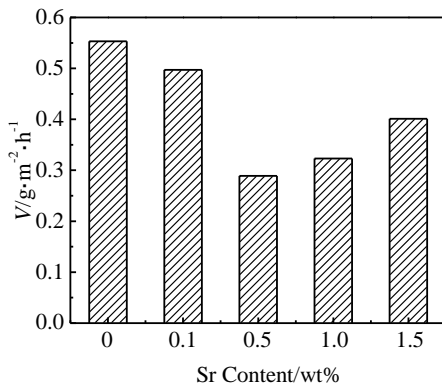


Fig.7 Corrosion rates of the experimental alloys

corrosion layer of the alloy is smoother and denser than those of other alloys. On the corrosion surface of the alloy with 1.0%~2.0% Sr, there are some exposed particles as shown in Fig.8d, 8f. According to the EDS results shown in Fig.9, the octahedral or blocks particles are Mg_2Si phase, while the long striped particles are $SrMgSi$ phase. Therefore, the surface of the alloy with 0.5%Sr undergoes milder corrosion than those of other alloys.

3 Discussion

3.1 Corrosion rate

Generally, the corrosion properties of magnesium alloy are influenced importantly by morphology and distribution of second phases or compounds depended on their volume and structure, which are due to their noble and stable during the corrosion process. It has been reported that Mg_2Si phase exhibits positive volta potential difference relative to the α -Mg matrix^[7]. So it was proposed that the Mg_2Si phases in the experimental alloys serve as a cathode, and many galvanic couples are formed between Mg_2Si and α -Mg matrix. As a result, they are effective initiation sites for the localized corrosion, which accelerate the corrosion rate of the alloys. The dissolution current density of anode (I_{a1}) or the galvanic current density (I_g) is well described by the theory of galvanic corrosion^[14]

$$\ln I_g = \ln I_{a1} = \frac{E_{\text{corr}2} - E_{\text{corr}1}}{b_{a1} + b_{c2}} + \frac{b_{a1}}{b_{a1} + b_{c2}} \ln I_{\text{corr}1} + \frac{b_{c2}}{b_{a1} + b_{c2}} \ln I_{\text{corr}2} + \frac{b_{c2}}{b_{a1} + b_{c2}} \ln \frac{A_2}{A_1} \quad (1)$$

where b_{a1} and b_{c2} are Tafel slopes of anodic reaction and cathodic reaction of anodic material, respectively; $E_{\text{corr}1}$ and $E_{\text{corr}2}$ are free corrosion potential of anode and cathode, respectively; $I_{\text{corr}1}$ and $I_{\text{corr}2}$ are free corrosion current of anode and cathode, respectively; A_1 and A_2 are area of anode and cathode, respectively.

Fortunately, the area ratio of Mg_2Si phase acted as cathode and α -Mg acted as anode in the present paper is much less than 1. That is,

$$A_1 \geq A_2 \quad (2)$$

$$0 \leq \frac{A_2}{A_1} \leq 1 \quad (3)$$

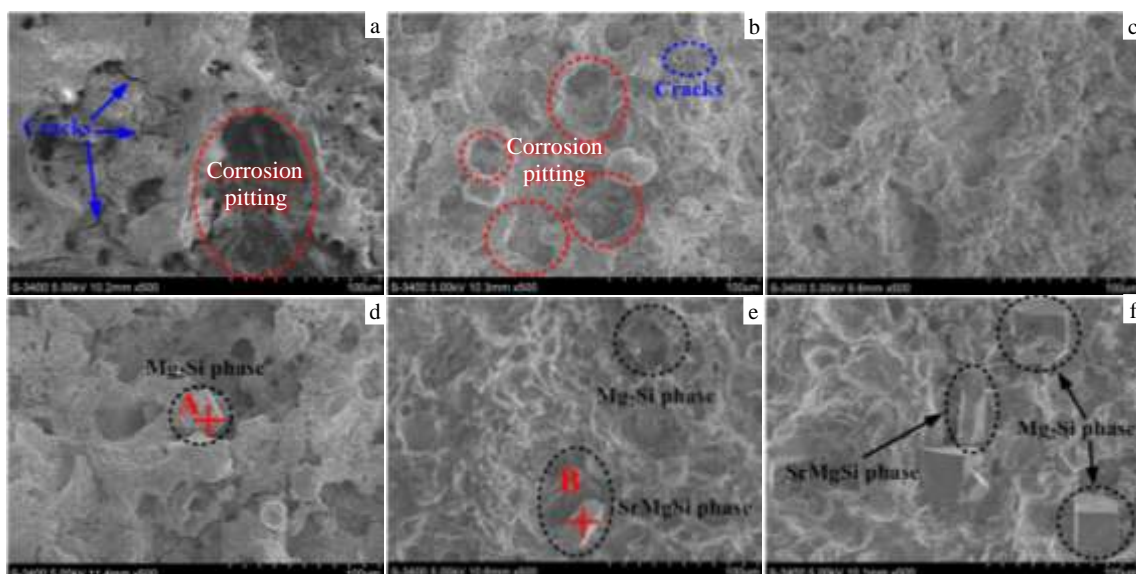


Fig.8 SEM images of the corroded surfaces of the experimental alloys: (a) without Sr, (b) 0.1% Sr, (c) 0.5% Sr, (d) 1.0% Sr, (e) 1.5% Sr, and (f) 2.0% Sr

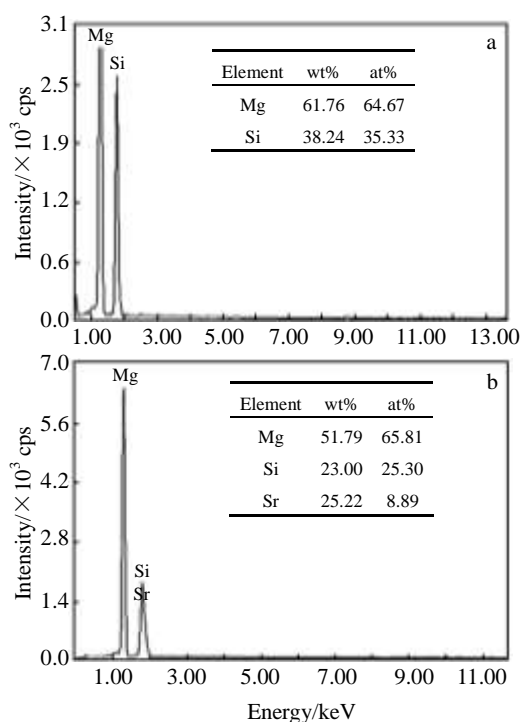


Fig.9 EDS results of points A and B in Fig.8d and 8e

$$\ln \frac{A_2}{A_1} \leq 0 \tag{4}$$

It can be concluded that the cathode to anode area ratio results in the reduction of I_g , and no-obvious worsening of the corrosion. Therefore, the smaller size of cathode phase is in favor of the corrosion resistance of the alloys, and it has been proved by Zhang et al. report where fine and evenly distributed polygonal shaped Mg_2Si phase with 1.6% Zn addition effectively impedes the corrosion process compared to the coarse Chinese script Mg_2Si in Mg-0.6Si alloy^[7]. In our experiments, after the addition of Sr, the size of Mg_2Si phases is refined and the distribution of Mg_2Si phase is uniform. The fine and evenly distributed Mg_2Si phases result in very weak pitting corrosion. Therefore, the corrosion rates of the alloys with Sr addition are reduced.

It is worth pointing out that the corrosion rate of the alloys increases with increasing Sr content from 0.5% to 1.0%~1.5%. In addition to the coarser size of Mg_2Si phases, needle-like SrMgSi phases may be also responsible for the increase of corrosion rate. Ben-Hamu et al. reported that the Volta potential difference relative to the magnesium matrix is 408.32 mV for CaMgSi intermetallic^[15]. Considering the similarity between the SrMgSi and CaMgSi intermetallics, it can be inferred that SrMgSi intermetallic alloy acts as a cathode with respect to the α -Mg matrix due to its positive volta potential difference. Consequently, the intermetallic becomes effective initiation sites for the localized corrosion, causing the decrease in corrosion resistance of Mg alloys. Additionally, Zhang et al. reported that the formation of new

polygonal and dot-shape CaMgSi phase causes the decrease in the contact area between the second phases and Mg matrix^[7], which leads to the reducing effect of galvanic couples. In the same way, SrMgSi phase reduces the effect of galvanic couples and the corrosion rate. Meanwhile, the coarser Mg_2Si phases promote corrosion behavior, and SrMgSi phases with higher potential relative to the matrix also accelerate the corrosion process. From the corrosion rate of the alloys with 0.5%Sr and 1.0%Sr, the positive influence of SrMgSi inducing the reduction of galvanic couples is smaller than the negative effect of SrMgSi and coarser Mg_2Si phases, and the corrosion rate of the alloy increases with the increasing of Sr element.

3.2 Corrosion morphology

It is well known that microstructure has important influences on corrosion resistance of magnesium alloys. According to the above description, the corrosion pits and cracks on the surface of the experimental alloys in Fig.8 reveal micro-galvanic corrosion between the Mg_2Si phase and its neighbouring α -Mg matrix. Zeng et al. reported that the intermetallic in Mg alloys exhibits relatively higher potential as cathode, and its neighboring α -Mg matrix acts as anode with a lower potential. In most cases as reported in literature, the big difference in potentials between the matrix and intermetallic leads to pitting corrosion^[16,17]. The Mg_2Si phases are effective initiation sites for the localized corrosion due to the formation of galvanic couples between Mg_2Si phases with α -Mg matrix, which accelerate the corrosion rate of the alloys. According to Chang et al., when the corrosion is initiated, α -Mg matrix dissolves, and evolution of hydrogen at the cathode happens simultaneously, which results in the formation of hydrogen gas^[18]. Meanwhile, $Mg(OH)_2$ is precipitated as the corrosion product on surface of samples. Along with the corrosion processes, the unit volumes of substrate and corrosion products are not inconsistent, and cause the mechanical stress^[19]. Meanwhile, hydrogen gas exists in the interfaces of the hydrides and Mg_2Si particles will cause high pressure in a local region^[20]. As the pressure of hydrogen is over a critical value, blisters formed inside the alloy may break and lead to the formation of cracks (marked by blue circles as shown in Fig.8). Thus, solution flows into internal matrix alloy along with the cracks, and promotes the corrosion process. Higher value of I_g , which is caused due to the coarse Mg_2Si phase, results in more severe corrosion. More mechanical stress is caused by unit volumes change quickly, and larger amounts of H_2 will be produced at the same time. Thus, blisters will rupture and lead to the formation of larger cracks. However, blisters is smaller and formed slowly as the Mg_2Si phase is refined. At the moment, small cracks, even no cracks appear. Besides that, the surface film is locally broken due to the mechanical stress and the pressure of hydrogen gas. Small pits are formed as the penetration of aggressive solution. Thus, primary Mg_2Si phase may falls out from the alloy due to the absence of support

from its neighboring α -Mg matrix, and leads to the formation of corrosion pits (marked by red circles as shown in Fig.8). With the addition of Sr increasing to 1.5% or 2.0%, large SrMgSi phase would increase the corrosion degree. The Mg₂Si or SrMgSi phase, which is perpendicular to the corrosion surface, will be exposed, and the phases paralleled to the surface will be corroded away (marked by black circles as shown in Fig.8).

4 Conclusions

1) A small amount of Sr addition leads to the changes in the morphology and grain size of the primary and eutectic Mg₂Si phase in the Mg-6Zn-4Si alloys, while the needle-like SrMgSi phase appears due to excessive Sr addition. The grain size of the primary Mg₂Si phase shows a minimum at the Sr addition of 0.5 wt%.

2) Due to the modification of the microstructure, the corrosion resistance of the Mg-6Zn-4Si alloys can be observably enhanced by Sr addition. The corrosion potential shifts significantly toward more noble position, and then toward negative with Sr addition. However, the current density of the experimental alloys decreases firstly, and gradually increases.

3) The Mg-6Zn-4Si-0.5Sr alloy exhibits the highest corrosion potential, the lowest corrosion current density and corrosion rate. The homogeneous dispersion of fine Mg₂Si particles with Sr element is responsible for the improvement of corrosion resistance.

References

- 1 Yuan G Y, Liu M P, Ding W J et al. *Materials Science and Engineering A*[J], 2003, 357: 314
- 2 Chen K, Li Z Q. *Journal of Alloys and Compounds*[J], 2014, 592: 196
- 3 Cong M Q, Li Z Q, Liu J S et al. *Journal of Alloys and Compounds*[J], 2012, 539: 168
- 4 De Negri S, Skrobanska M, Saccone A et al. *Intermetallics*[J], 2010, 18: 1722
- 5 Asano K, Yoneda H. *Materials Transactions*[J], 2007, 48: 1469
- 6 Evangelista E, Gariboldi E, Lohne O et al. *Materials Science and Engineering A*[J], 2004, 387-389: 41
- 7 Zhang E L, Yang L, Xu J W et al. *Acta Biomaterialia*[J], 2010, 6(5): 1756
- 8 Wang L P, Guo E J, Ma B X. *Rare Earths*[J], 2008, 26: 105
- 9 Çiçek B, Ahlatçı H, Sun Y. *Materials & Design*[J], 2013, 50(17): 929
- 10 Alizadeh R, Mahmudi R. *Journal of Alloys and Compounds*[J], 2011, 509: 9195
- 11 He X, Chen J H, Yan H G et al. *Journal of Alloys and Compounds*[J], 2013, 579: 39
- 12 Zhang Y C, Yang L, Dai J et al. *Materials Science and Engineering A*[J], 2014, 610: 309
- 13 Cong M Q, Li Z Q, Liu J S et al. *Materials & Design*[J], 2014, 53: 430
- 14 Cao C N. *Corrosion Electrochemistry*[M]. Beijing: Chemistry Industry Press, 2008: 105
- 15 Ben-Hamu G, Eliezer D, Shin K S. *Materials Science and Engineering A*[J], 2007, 447: 35
- 16 Zeng R C, Zhang J, Huang W J et al. *Transactions of Nonferrous Metals Society of China*[J], 2006, 16: s763
- 17 Song G, Atrens A. *Advanced Engineering Materials*[J], 1999, 1: 11
- 18 Chang D Y, Jie Y, Sang K W et al. *Corrosion Science*[J], 2015, 90: 597
- 19 Chen J, Ai M, Wang J et al. *Corrosion Science*[J], 2009, 51: 1197
- 20 Kappes M, Iannuzzi M, Carranza R M. *Journal of the Electrochemical Society*[J], 2013, 160: C168

Sr 添加 Mg-6Zn-4Si 铸态合金的腐蚀行为研究

丛孟启¹, 李子全^{1,2}, 刘劲松¹, 王梦慧¹, 盛备备¹, 王碧军¹

(1. 南京航空航天大学, 江苏 南京 210016)

(2. 南京科技职业学院, 江苏 南京 210048)

摘要: 利用 XRD、OM、SEM、EDS、极化曲线测试和浸泡试验分析研究 Sr 元素添加 Mg-6Zn-4Si 铸态合金的显微结构和腐蚀行为。Sr 元素的添加能够有效地改善 Mg-6Zn-4Si 合金中初生及共晶 Mg₂Si 相的形貌和尺寸。随着 Sr 元素添加量的增加, 初生 Mg₂Si 相的尺寸先降低后逐渐增加。Sr 元素能够有效地改善合金的耐腐蚀性。当 Sr 添加量为 0.5% (质量分数) 时, 合金具有最优的耐蚀性, 此时表现为最高的腐蚀电位, 最低的腐蚀电流密度和腐蚀速率。添加 Sr 元素后, 细小且分散均匀的 Mg₂Si 相是耐蚀性提高的主要原因。过量的 Sr 添加会形成针状 SrMgSi 新相, 降低了合金的耐蚀性。

关键词: 镁合金; 铸造; 显微结构; 腐蚀行为

作者简介: 丛孟启, 男, 1987 年生, 博士生, 南京航空航天大学材料科学与技术学院, 江苏 南京 210016, E-mail: mqcong@nuaa.edu.cn